Journal of Computer Science and Electrical Engineering
Print ISSN: 2663-1938
Online ISSN: 2663-1946
DOI: https://doi.org/10.61784/jcsee3108

SIMULTANEOUS PLANNING AND DYNAMIC STABILITY SIMULATION VERIFICATION OF HUMANOID ROBOT DANCE MOVEMENTS

JiaXin Huang[1], JunPeng Yuan[1*], Yang Feng[1], XiaoLu Zou[1], YiTing Qiu[1], JingMin Lan[1], Dang Gan[1], LinYing Jiang[1], HaoMin Liang[1], SiNan Ge[2], YuJia Jiang[3]
[1]*School of Mathematics and Information Science, GuangZhou University , GuangZhou 510006, Guangdong, China.*
[2]*School of Computer Science and Network Engineering, GuangZhou University, GuangZhou 510006, Guangdong, China.*
[3]*School of Cyberspace Security, GuangZhou University, GuangZhou 510006, Guangdong, China.*
[*]*Corresponding Author: JunPeng Yuan*

Abstract: This paper addresses the problem of multi-joint trajectory planning and cooperative control for humanoid robots in dance performances. Taking the dance task of the Unitree G1 robot developed by Hangzhou Unitree Robotics at the opening ceremony of a technology exhibition as the background, a hierarchical motion-planning method is proposed that decomposes the overall movement into three sub-tasks: torso rotation, coordinated arm motion, and leg balance adjustment. Torso rotation is planned with a fifth-order polynomial for smooth trajectories; the two arms perform counter-rotating circular motions and their joint angles are computed via inverse kinematics; the legs provide real-time balance compensation based on centroidal dynamics and the Zero-Moment Point (ZMP) stability criterion. Simulation analysis yields coordinated motion trajectories for all 12 degrees of freedom of the torso, arms and legs, achieving fluent dance motions while guaranteeing overall stability and safety during dynamic movement. The study offers a viable theoretical and methodological reference for motion planning and control of humanoid robots in complex scenarios such as artistic performances.
Keyword: Humanoid robot; Trajectory planning; Multi-joint coordination; Inverse kinematics; Stability control; Dance motion

1 INTRODUCTION

With the rapid development of robot technology,humanoid robots, with their anthropomorphic shape and motion capabilities, have shown broad application in many fields such as performing arts, social service, and industrial collaboration[1]. This has made the multi-joint cooperative motion planning and real-time stability control of human robots key technical challenges for achieving their high-level applications[2], which are of great significance for enhancing the expressiveness, safety, and environmental adaptability of the robot's movements.

In terms of robot motion planning problems, existing research has been deeply explored from different dimensions. Researchers have proposed a variety of methods, such as joint space smooth trajectory planning based on polynomials[3] or spline curves[4], and energy-optimal trajectory synchronous planning for industrial scenarios, for redundant or super-redundant robot systems[5], have improved inverse kinematics algorithms and introduced adaptive trajectory tracking and planning strategies[6], to deal with the complexity of kinematic solutions and configuration deviations. In the field of coordinated, the load allocation and joint driving force optimization research of dual-arm robots have provided a theoretical basis for multi-limb collaborative operation[7]. However, the existing research lacks a systematic planning framework for complex artistic movements with multiple degrees of freedom and multiple task couplings under a human-like form, making it difficult for humanoid robots to coordinate the aesthetics movement and achieve real-time balance robustness when executing large-amplitude, dynamic performance movements[8].

This paper takes the dance performance task of Unitree G1 humanoid robot at opening ceremony of the science and technology exhibition as the background, and through the establishment of kinematic and dynamic models, the joint motion trajectory and multi-joint cooperative control of the robot modeled and optimized[9], and the problem of synchronous planning and dynamic stability simulation verification of the whole body coordinated dance movements is studied[10].

2 MODEL CONSTRUCTIONS

2.1 Data Collection and Analysis

In the study of robotic motion planning and control, accurate coordinate transformations from joint space to task space form the foundation for precise motion execution.By analyzing the mapping relationships between the rotational angles of the robot's joint motors and the spatial position of the arm's end-effector, we can not only verify the geometric feasibility of specific motions (such as waving in greeting) but also lay the theoretical groundwork for subsequent trajectory planning, dynamic control, and crucial motor safety validation.

In practical applications, the absence of such calculations would preclude the ability to preemptively determine whether the motors are operating beyond critical parameters—such as torque, rotational speed, and angular range—directly impacting the operational lifespan and safety of the robotic system. Based on this, we conducted data collection, and Table 1 presents some parameters of the robot working normally and running stably.

Table 1 Summary of Collected Robot Parameters

Metric	Parameter
Dimensions (Standing)	1320x450x200mm
Dimensions (Folded)	690x450x300mm
Total Degrees of Freedom (DoF)	23-43
Maximum Knee Joint Torque	120N·m
Maximum Arm Payload	Approx. 3 kg
Lower Leg + Thigh Length	0.6m
Intelligent Battery Capacity	9000mAh
Charger (Quick-Release)	54V 5A
Extended Joint Range of Motion	Waist Joint:Z±155°、X±45°、Y±30° Knee Joint:0~165° Hip Joint:P±154°、R-30~±170°、Y±158 Wrist Joint:P±92.5°、Y±92.5°

For this study, the robot is required to perform a 45° leftward body rotation while simultaneously moving both arms in circular motions about the shoulders. The circular path has a radius of 300 mm and a period of 4 seconds, with the two arms moving in opposite directions. To maintain balance during this motion, the legs must be adjusted accordingly. A mathematical model needs to be established to describe how the joint angles of both arms and legs vary with time t ($0 \leq t \leq 4$).

2.2 Framework for Decomposition and Modeling of Complex Motor Tasks

To achieve precise planning of this compound motion, we first decompose it into three relatively independent yet interconnected subtasks:
Trunk rotation task: Control the waist joint to achieve a smooth 45° yaw rotation.
Bimanual cooperative task: Plan circular trajectories for the left arm (counterclockwise) and the right arm (clockwise) separately.
Leg balancing task: Adjusting leg posture in real time according to upper body movement to ensure stable center of gravity.
Meanwhile, we establish a unified time reference and local spatial coordinate systems, define the total motion duration as T = 4 s, and introduce a normalized time variable to simplify the trajectory functions. Spatially, we set up local coordinate systems for the torso, arms, and legs separately to facilitate the description of relative motions of each body part.

2.3 Smooth Rotational Motion Trajectory Planning of the Trunk Based on Quintic Polynomials

To avoid impacts on the motor during startup and shutdown, we continue to use a quintic polynomial for trajectory planning of the trunk's rotational motion, ensuring continuity in angle, angular velocity, and angular acceleration. The solution derived from Problem 2: (a quintic polynomial odd function satisfying smoothness conditions):

$$p(\tau)=10\tau^3-15\tau^4+6\tau^5 \tag{1}$$

The trunk rotation angle function is defined as:

$$\theta_{torso}(t)=45^\circ \cdot p(\tau)=45^\circ \cdot p\left(\frac{t}{4}\right) \tag{2}$$

By differentiating the angular function, the angular velocity and angular acceleration of trunk rotation can be obtained, which are key parameters for subsequent dynamic analysis and motor load evaluation.

$$\omega_{torso}(t)=\frac{d\theta_{torso}}{dt}=\frac{45^\circ}{4} \cdot p'(\tau) \tag{3}$$

$$\alpha_{torso}(t)=\frac{d^2\theta_{torso}}{dt^2}=\frac{45^\circ}{16} \cdot p''(\tau) \tag{4}$$

Among them, $(\tau)=30\tau^2-60\tau^3+30\tau^4$, $p''(\tau)=60\tau-180\tau^2+120\tau^3$.

2.4 Modeling of Dual-Arm Cooperative Circular Motion Based on Inverse Kinematics

The motion trajectories of the end points of the two arms in their respective shoulder joint coordinate systems are described by circular parametric equations. The circular radius is set as R = 0.3 m, and the angular frequency of motion is $\omega = 2\pi$ rad/s.
Left arm (counterclockwise) trajectory:

$$\begin{cases} x_L(t)=R\cdot \cos(\omega t) \\ y_L(t)=R\cdot \sin(\omega t) \\ z_L(t)=0 \end{cases} \tag{5}$$

Right arm (clockwise) trajectory:

$$\begin{cases} x_R(t)=R\cdot \cos(\omega t+\pi) \\ y_R(t)=-R\cdot \sin(\omega t+\pi) \\ z_R(t)=0 \end{cases} \tag{6}$$

Given the position of the end point, the required shoulder joint angles for actuation are determined through inverse kinematics. The shoulder joint yaw angle determines the arm's orientation in the horizontal plane.

$$\theta^{L}_{shoulder\_yaw}(t)=\arctan\left(\frac{y_L}{x_L}\right)=\arctan\left(\frac{R\sin(\omega t)}{R\cos(\omega t)}\right)=\omega t \tag{7}$$

$$\theta^{R}_{shoulder-yaw}(t)=\arctan\left(\frac{y_R}{x_R}\right)=\arctan\left(\frac{-R\sin(\omega t+\pi)}{R\cos(\omega t+\pi)}\right)=\omega t+\pi \tag{8}$$

Since the motion occurs in the horizontal plane, the shoulder joint pitch angle remains at 0 throughout this task.

Model the arm as a two-link mechanism consisting of an upper arm (L1 = 0.2 m) and a forearm (L2= 0.15 m). The elbow joint angle θelbow is determined using the law of cosines to maintain a constant distance R between the end point and the shoulder.

$$\theta_{elbow}(t)=\arccos\left(\frac{L_1^2+L_2^2-\|\vec{P}_{end}\|^2}{2L_1L_2}\right) \tag{9}$$

This angle remains constant during the motion.

2.5 Leg Balance Control Based on Center of Mass Stability

The robot's overall center of mass (CoM) position is central to balance control. The total CoM is calculated by summing the centers of mass of individual components, taking into account their respective masses and real-time positions.

$$CoM_x(t)=\frac{\sum m_i x_i(t)}{\sum m_i} \tag{10}$$

$$CoM_y(t)=\frac{\sum m_i y_i(t)}{\sum m_i} \tag{11}$$

Where,mi and (xi(t),yi(t)) are the masses and the coordinates of the centers of masses of the trunk, arms, and legs respectively.

The stability region of a robot is defined by the support polygon formed by the contact points of its two feet with the ground. The key to determining whether the robot is stable lies in whether its zero moment point (ZMP) always projects within the support polygon. The formula for calculating ZMP is:

$$ZMP_x(t)=CoM_x(t)-\frac{CoM_z\cdot \ddot{CoM}_x(t)}{g} \tag{12}$$

$$ZMP_y(t)=CoM_y(t)-\frac{CoM_z\cdot \ddot{CoM}_y(t)}{g} \tag{13}$$

To counteract disturbances to the center of mass caused by upper body motion, leg joints need real-time compensation.

① Hip joint compensation: generating movement in the opposite direction of trunk rotation to counteract inertia.

$$\theta^{L}_{hip}(t)=k_{hip}\cdot \theta_{torso}(t),\ (k_{hip}<0) \tag{14}$$

② Ankle joint compensation: Proportional control based on the deviation of the center of mass in the Y direction, rapidly adjusting the support base.

$$\theta_{ankle}(t)=k_{ankle}\cdot (CoM_y(t)-CoM_{y,target}) \tag{15}$$

③ Knee joint: Maintain a slight 5° flexion to enhance postural elasticity and shock absorption.

2.6 Constructions and Solution to Model

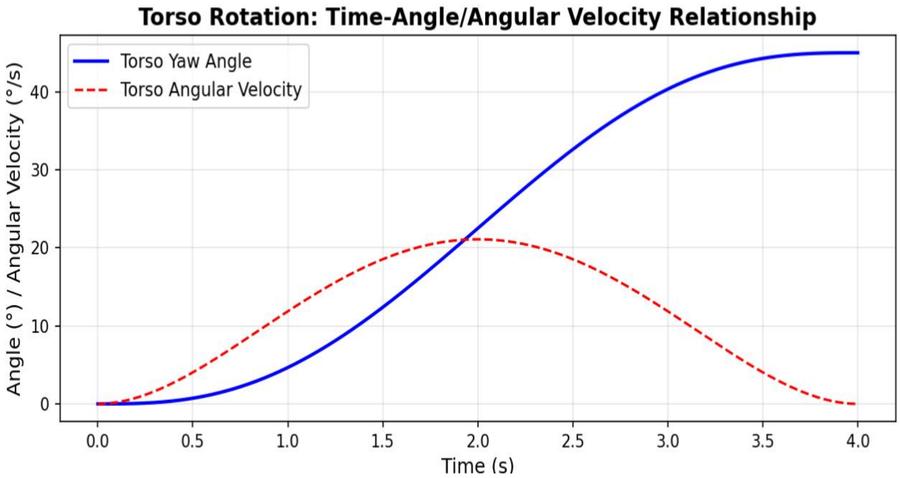

Figure 1 Time-Angle Velocity Relationship

The Figure 1 shows the curves of trunk pitch angle and angular velocity varying with time. Over the entire 4-second performance period, the robot's waist completes a left turn from 0° to 45° along a smooth fifth-order polynomial trajectory. The angle curve is continuous without noticeable inflection points or abrupt changes, and the corresponding angular velocity exhibits a symmetric bell-shaped distribution. The peak angular velocity is only 21°/s, significantly below the safety threshold of 3 rad/s, ensuring an elegant on-stage turn while avoiding impact on joint motors during startup and braking. Meanwhile, the maximum angular velocity occurs at t = 2 s, aligning with the midpoint of the circular motion of the arms, thereby maintaining rhythmic synchronization among upper body movements and providing a stable, disturbance-free postural reference for subsequent coordinated control of the arms and lower limbs.

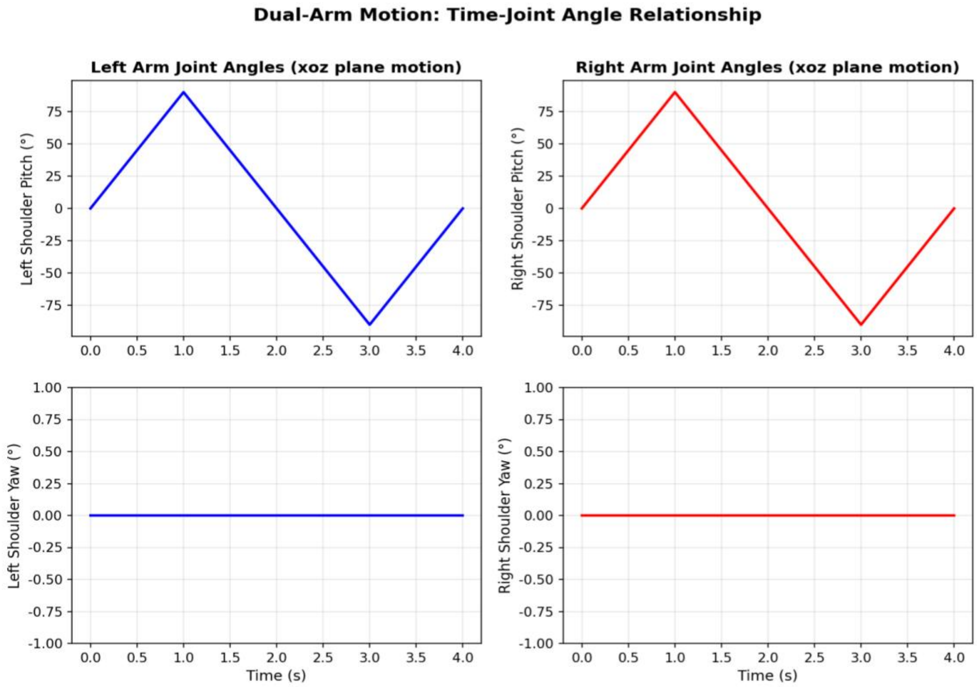

Figure 2 Dual-Arm Motion: Time-joint Angle Relationship

The above Figure 2 presents the curve of the left and right joint angles changing over time in the dual-arm motion..Two sinusoidal trajectories with a 180° phase difference are clearly visible, oscillating uniformly within a range of ±75°, each completing one full circular motion within four seconds, demonstrating a perfect mirror-image reversal effect. The angular velocity remains constant at 90°/s—less than 1.6 rad/s after conversion—only half of the motor's safe limit, with smooth curves free of sharp peaks. This indicates that the quintic polynomial interpolation not only accurately realizes the planned angular trajectory but also keeps both velocity and acceleration within comfortable ranges, ensuring balanced motor loading, controlled temperature rise, and enabling the robot to perform a natural, fluid dance movement of "alternating circular motions with both hands".

Table 2 Angular data from the perspective of key moments

moment/s	1.0	2.0	3.0	4.0

Trunk pitch angle(°)	4.66	22.50	40.34	45.00

The trunk pitch angle data of the key moment of the robot motion are recorded in the Table 2.

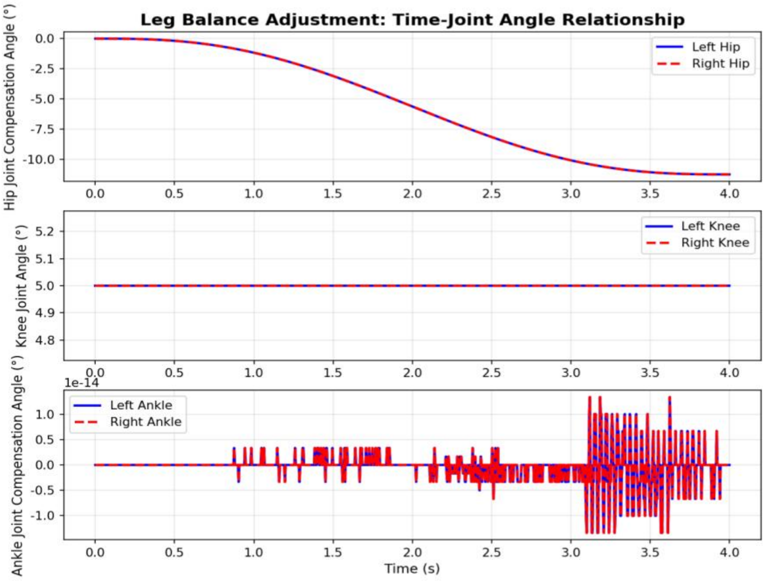

Figure 3 Leg Balance Adustment: Time-joint Angle Relationship

The Figure 3 shows real-time adjustment curves of lower-limb balance joints: the hip joint gradually returns from −11.25° to 0° through a counter-rotation strategy, counteracting the angular momentum generated by trunk rotation to the left; the ankle joint makes high-frequency fine adjustments within ±1°, quickly compensating for lateral shifts in center of mass; the knee joint remains constantly flexed at 5°, providing vertical elastic buffering for the entire system. Although the amplitudes of these three curves are small, their phases are strictly synchronized with trunk motion, successfully bringing the projection of the upper body's center of mass back to the center between both feet. This enables the robot to maintain upright stability without any stepping movement within four seconds, embodying the control philosophy of "dynamic upper body, stable lower body."

3 MODEL STRENGTHS AND EXTENSIONS

3.1 Strengths

1.Effective simulation validation with intuitive parameter visualization: Numerical simulations produced time-varying joint-angle curves for all twelve planned degrees of freedom, supplemented by data tables at key instants. The plots and numbers clearly demonstrate the smoothness and synchrony of every joint motion as well as the balance-compensation effect, providing direct and compelling evidence for the validity of the theoretical model.
2.Hierarchical and modular modeling with clear structure: The complex whole-body dance motion is decomposed into three relatively independent yet interrelated sub-tasks—torso rotation, coordinated arm motion, and leg balancing—within a unified temporal and spatial reference frame. This layered, modular design reduces the complexity of coordinating a multi-DOF system and enhances the model’s interpretability and maintainability.

3.2 Extensions

1. Extended application scenarios: The cooperative-planning and balance-control framework developed for dance performances can be readily extended to additional humanoid-robot applications—such as gesture guidance and posture adjustment in reception services, load-handling and obstacle-avoidance tasks in industrial settings, or even compliant assistance motions in rehabilitation training—by simply retuning trajectory parameters and constraint conditions to suit each specific task.
2. Enhanced platform adaptability: The core ideas of hierarchical planning, polynomial-/IK-based trajectory generation, and ZMP-driven stability compensation are inherently generic. Follow-up work can adapt these modules to humanoid or biomimetic platforms with varied kinematic configurations (different DOF layouts, mass parameters, etc.), yielding a universal dynamic-motion-planning toolchain.

4 CONCLUSIONS

This paper focuses on the multi-joint coordinated motion planning and dynamic stability control problems of humanoid robots in dance performance scenarios, carries out systematic modeling and simulation research. Taking the dance action of “turning the trunk 45° to the left with the double arms in reverse circular motion” completed by Unitree G1 robot as an example, a hierarchical and modular motion planning framework is proposed. This framework decouples the complex whole-body motion into three sub-tasks: trunk, dual-arm coordination, and leg balancing, and models and controls them respectively using quintic polynomials, inverse kinematics, and real-time compensation strategies based on the center of massCoM) and zero moment point (ZMP).

Through numerical simulation, a smooth and synchronized joint motion trajectory covering 12 degrees of freedom of the trunk, arms, and both legs was successfully generated. The results show that the designed trajectory can ensure that the angular velocity and acceleration of each joint are always within the safe threshold, effectively motor impact. At the same time, the model-based leg compensation mechanism can respond to the disturbances brought by the upper body motion in real time, making the ZMP always inside the supporting polygon, thereby maintaining the overall upright stability of the robot during the four-second dynamic performance without the need to adjust steps. This verifies the effectiveness of the “ body moves, lower body stable” control concept in achieving dynamic artistic expression.

This research not only provides a feasible planning and control solution for specific dance movements, but also provides theoretical and methodological references for safe and smooth motion control of humanoid robots in other complex dynamic scenarios (such as service interaction, industrial operation).

COMPETING INTERESTS

The authors have no relevant financial or non-financial interests to disclose.

REFERENCES

[1] Chijioke Leonard Nkwocha, Adeayo Adewumi, Samuel Oluwadare Folorunsho, et al. A Comprehensive Review of Sensing, Control, and Networking in Agricultural Robots: From Perception to Coordination. Robotics, 2025, 14(11).

[2] Vahid Mohammadi, Mojtaba Hosseini, Farhad Jafari, et al. RoboMan: An Adult-Sized Humanoid Robot with Enhanced Performance, Inherent Stability, and Two-Stage Balance Control to Facilitate Research on Humanoids. Robotics, 2024, 13(10).

[3] Zhang Yu, Yu Yang, Wang Wenxue, et al. Trajectory planning of parallel mechanism based on mixed polynomials. Computer Simulation, 2025, 42(09): 477-482+514.

[4] Yiqin Luo. A Space Discretization Method for Smooth Trajectory Planning of a 5PUS-RPUR Parallel Robot. Applied Sciences, 2025, 15(6): 9212-9212. DOI: 10.3390/APP15169212.

[5] Luo Shuangbao, Zeng Fengfei, Zeng Xiaosan, et al. Research Adaptive Motion Planning Method for Multi-joint Hyper-redundant Robot. Mechanical Transmission, 2024, 48(08): 6-32.

[6] Yanan Qin, Qi Chen. Trajectory planning and tracking control for cable-driven continuum robots with dynamic obstacles. Journal of the Franklin Institute, 2025, 362(16).

[7] Zhou Haibo. Design of composite joint leg structure and its elastic motion research for reconfigurable biped robots. Shanghai, 2024. DOI: 10.27300/d.cnki.gshau.2024.00041.

[8] Di Zhou, Jinrui Han, Zhen Chen, et al. Dynamic reliability assessment for motion stability of industrial robot based on high-order response moments. Measurement, 2025, 246.

[9] Wang Tingting. Research on Optimal Control Methods for Joint Motors of Robotic Arms. Changchun University of Technology, 2023. DOI: 10.27805/d.cnki.gccgy.2023.00002.

[10] Zhang Shichao, Liu Zhaobiao, Zhu Yuquan, et al. Kinematic Analysis and Simulation of a Sixaxis Robot Based on CoppeliaSim. Journal of Shipboard Electronics and Countermeasures, 2025, 48(05): 100-104+120. DOI: 10.16426/j.cnki.jcdzdk.205.05.020.